

SUPPORTING INFORMATION

Generation and transformation of a hemi-iminal-based metal-organic Fe(II) structure obtained via subcomponent self-assembly in water

Grzegorz Markiewicz,^{a,b} Miłosz Piechocki,^{a,b} Anna Walczak,^{a,b} Ewa A. Połomska,^{a,b} Jack

Harrowfield^c and Artur R. Stefankiewicz^{a,b*}

a Faculty of Chemistry, Adam Mickiewicz University, ul. Umultowska 89b, 61-614 Poznań, Poland.

b Center for Advanced Technologies, Adam Mickiewicz University, ul. Umultowska 89c, 61-614 Poznań.

c ISIS, Université de Strasbourg, 8 allée Gaspard Monge, 67083 Strasbourg, France

* E-mail: ars@amu.edu.pl

Contents

1. NMR data	S2
2. Mass Spectrometry Data	S6
3. UV-Vis data	S9
4. Elemental Analysis data.....	S9
5. Crystallographic data	S10
6. Supplementary References.....	S11

1. NMR data

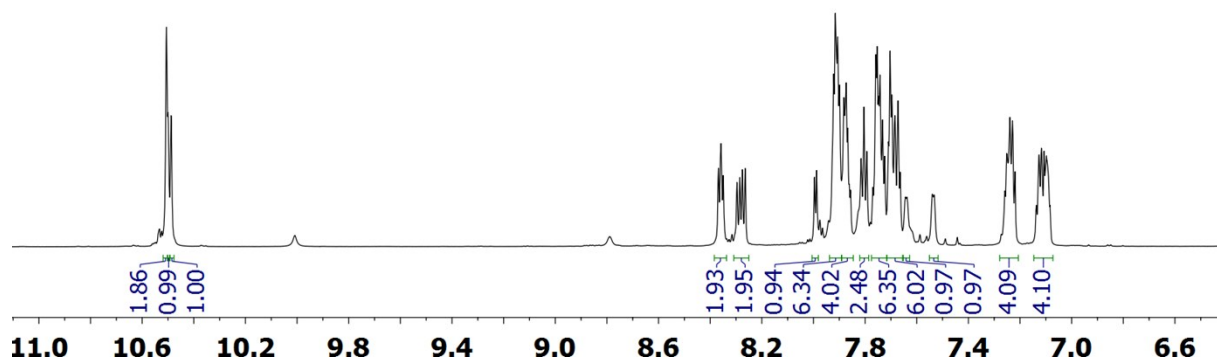


Figure S1. ^1H NMR (700 MHz CD_3CN) spectrum of $[\text{Fe}^{\text{II}}(\text{L})_2](\text{ClO}_4)_2$.

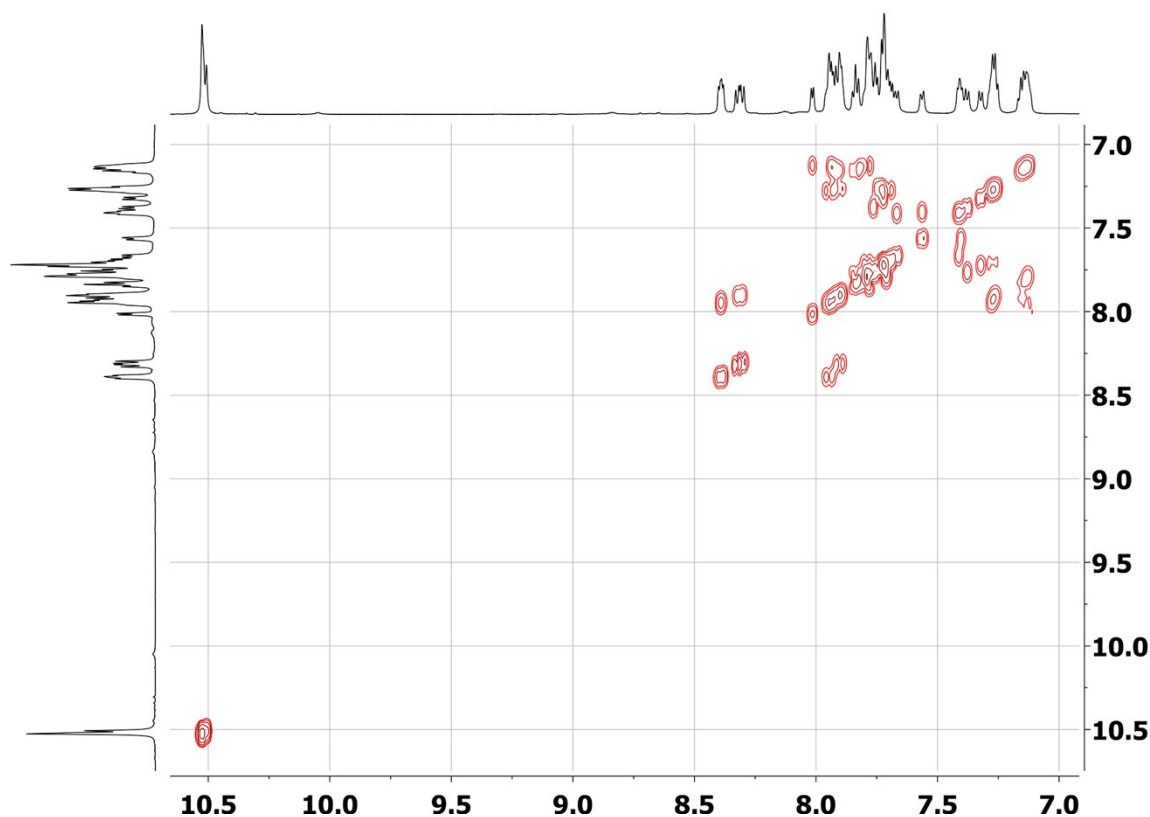


Figure S2. COSY NMR (600 MHz CD_3CN) spectrum of $[\text{Fe}^{\text{II}}(\text{L})_2](\text{ClO}_4)_2$.

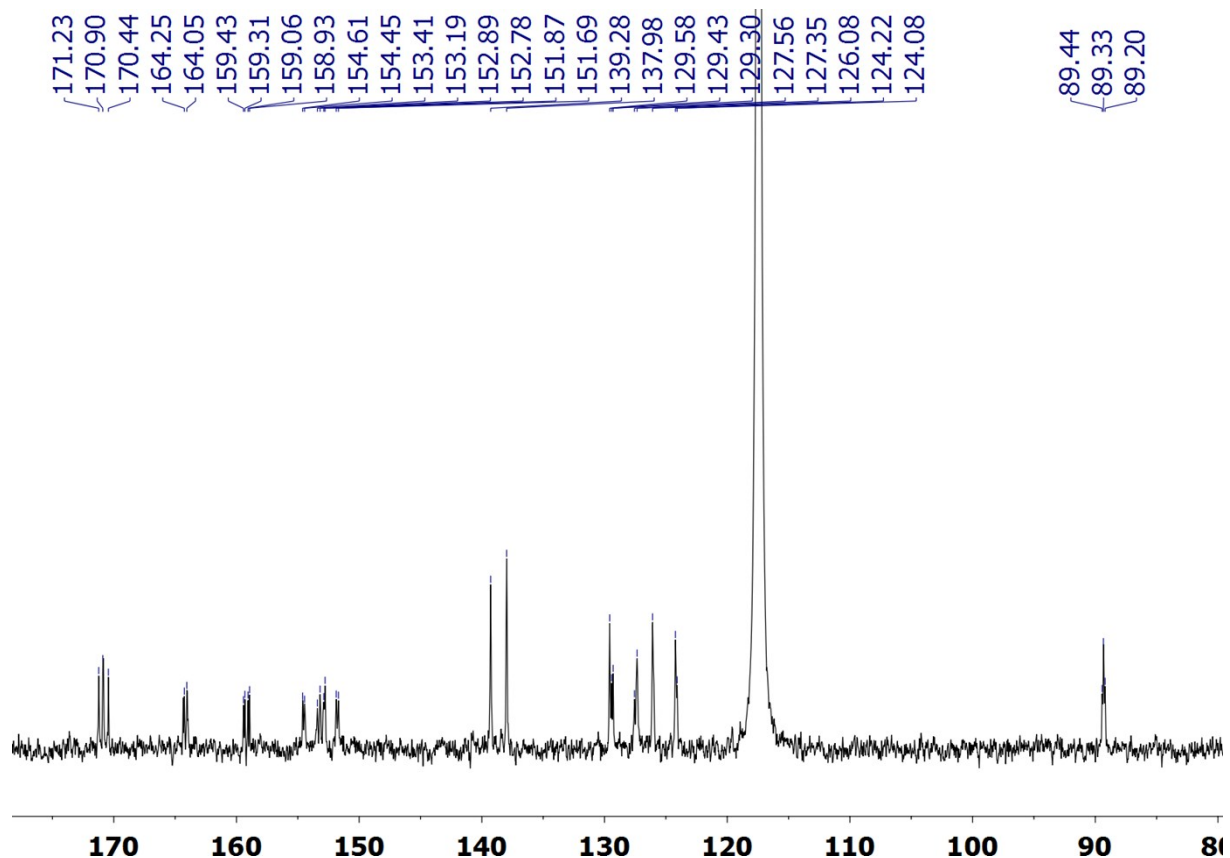


Figure S3. ^{13}C NMR (75 MHz CD_3CN) spectrum of $[\text{Fe}^{\text{II}}(\text{L})_2](\text{ClO}_4)_2$.

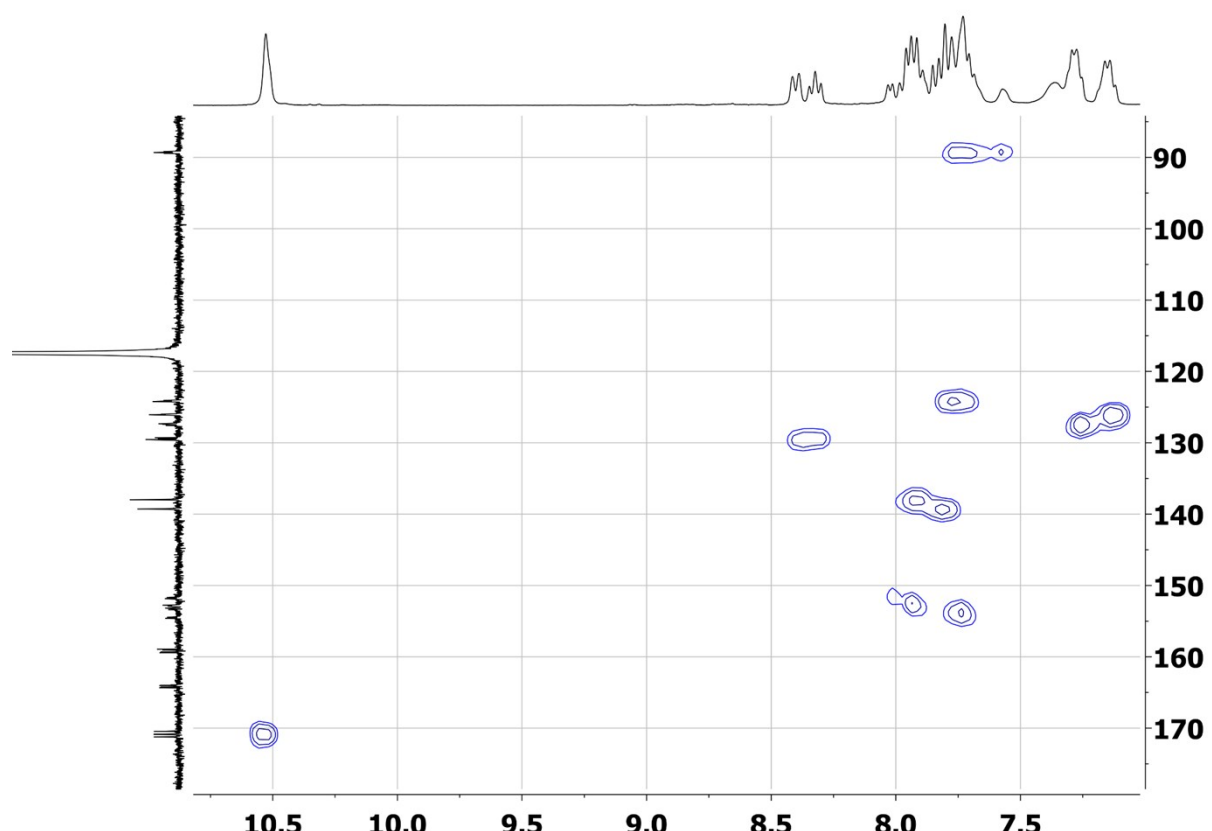


Figure S4. ^1H - ^{13}C HSQC NMR (300/75 MHz CD_3CN) spectrum of $[\text{Fe}^{\text{II}}(\text{L})_2](\text{ClO}_4)_2$

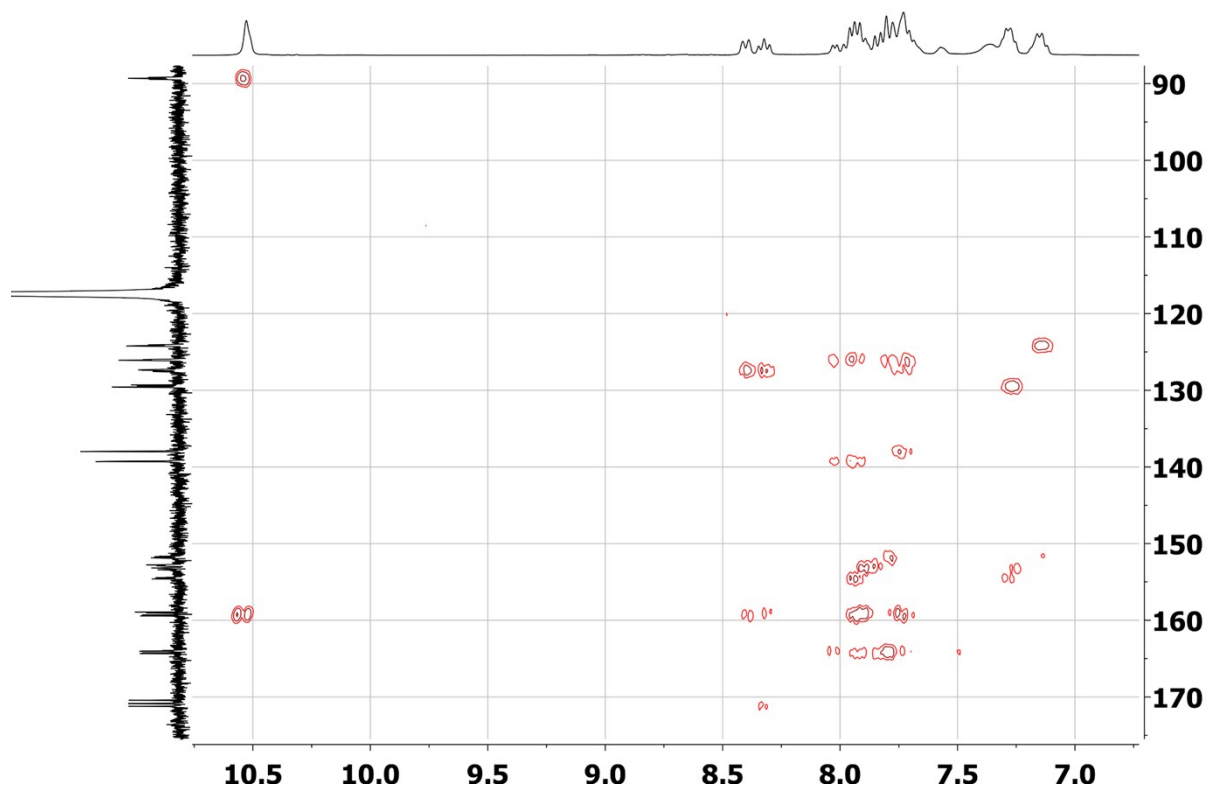


Figure S5. ^1H - ^{13}C HMBC NMR (300/75 MHz CD_3CN) spectrum of $[\text{Fe}^{\text{II}}(\text{L})_2](\text{ClO}_4)_2$

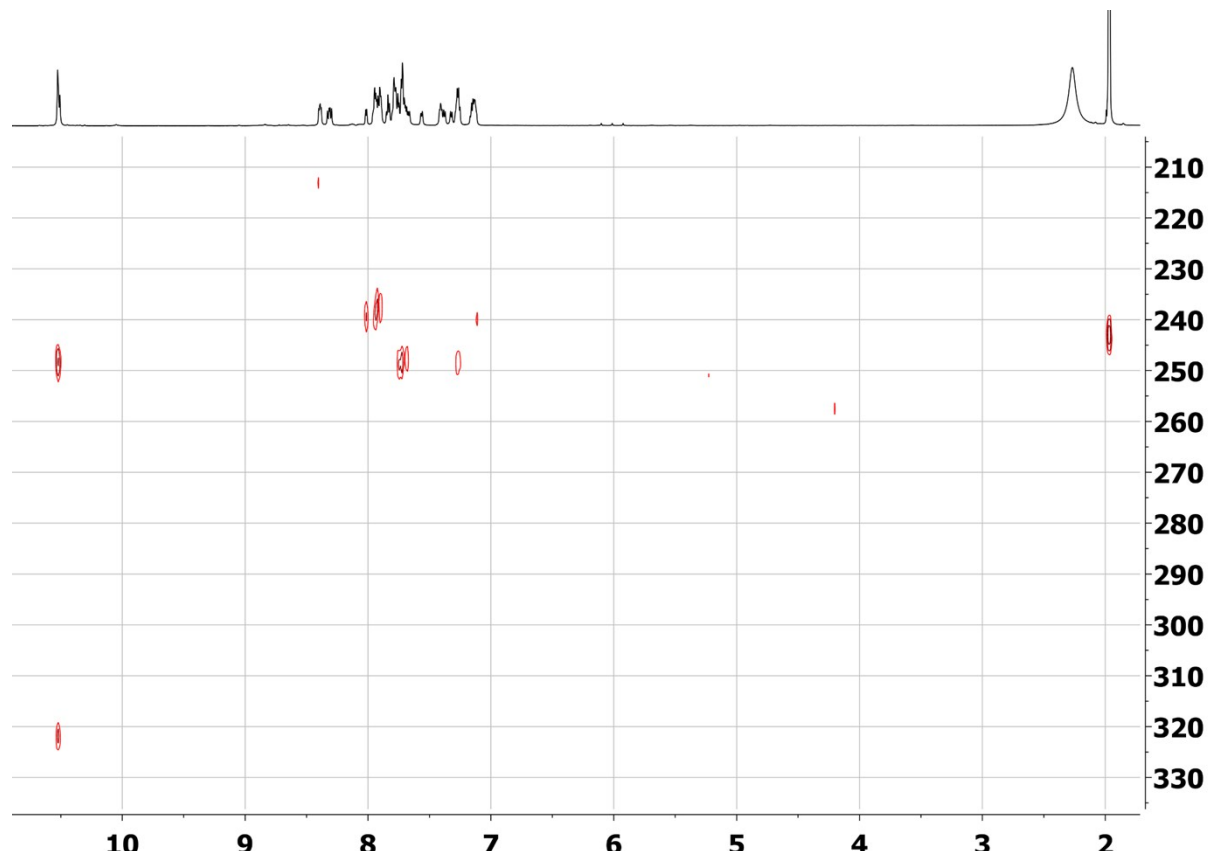


Figure S6. ^1H - ^{15}N HMBC NMR (600/60 MHz CD_3CN) spectrum of $[\text{Fe}^{\text{II}}(\text{L})_2](\text{ClO}_4)_2$

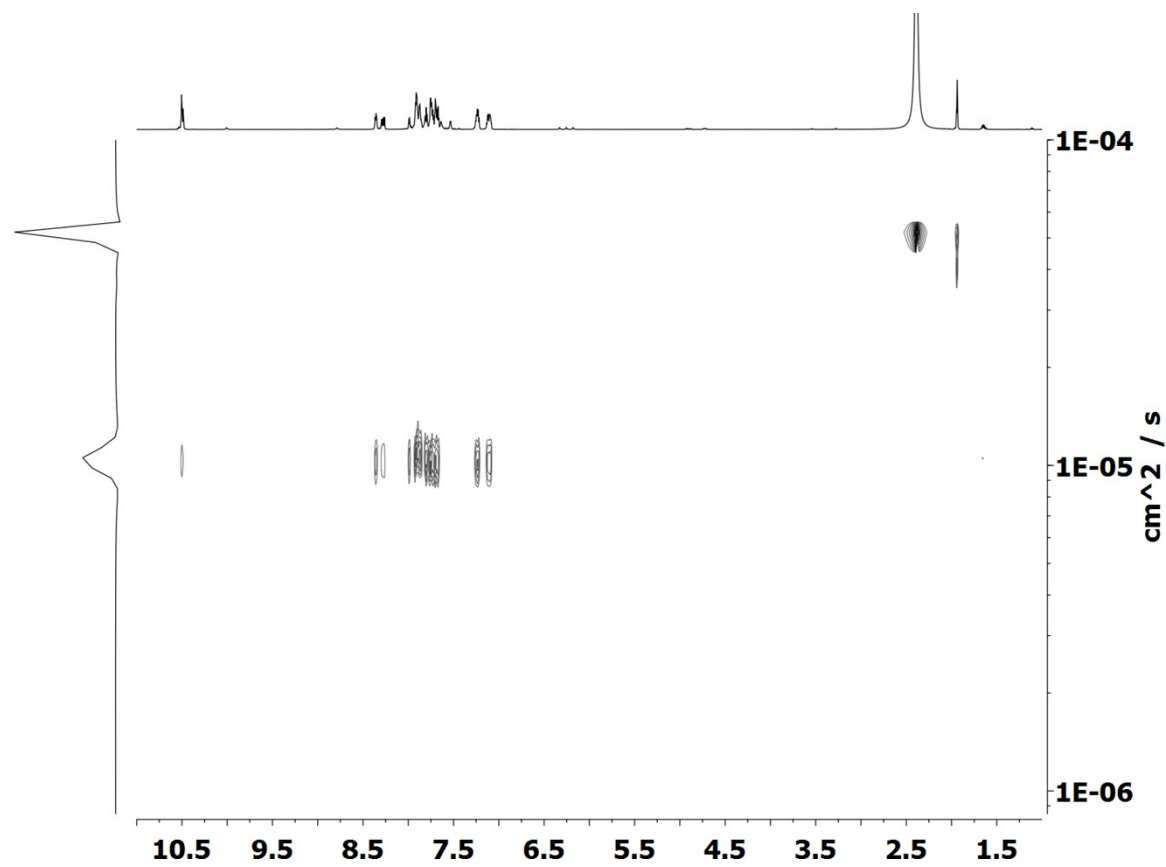


Figure S7. ^1H DOSY NMR (700 MHz, CD_3CN) spectrum of $[\text{Fe}^{II}(\text{L})_2](\text{ClO}_4)_2$. Observed diffusion coefficient $D=1.02 \cdot 10^{-9} \text{ m}^2/\text{s}$.

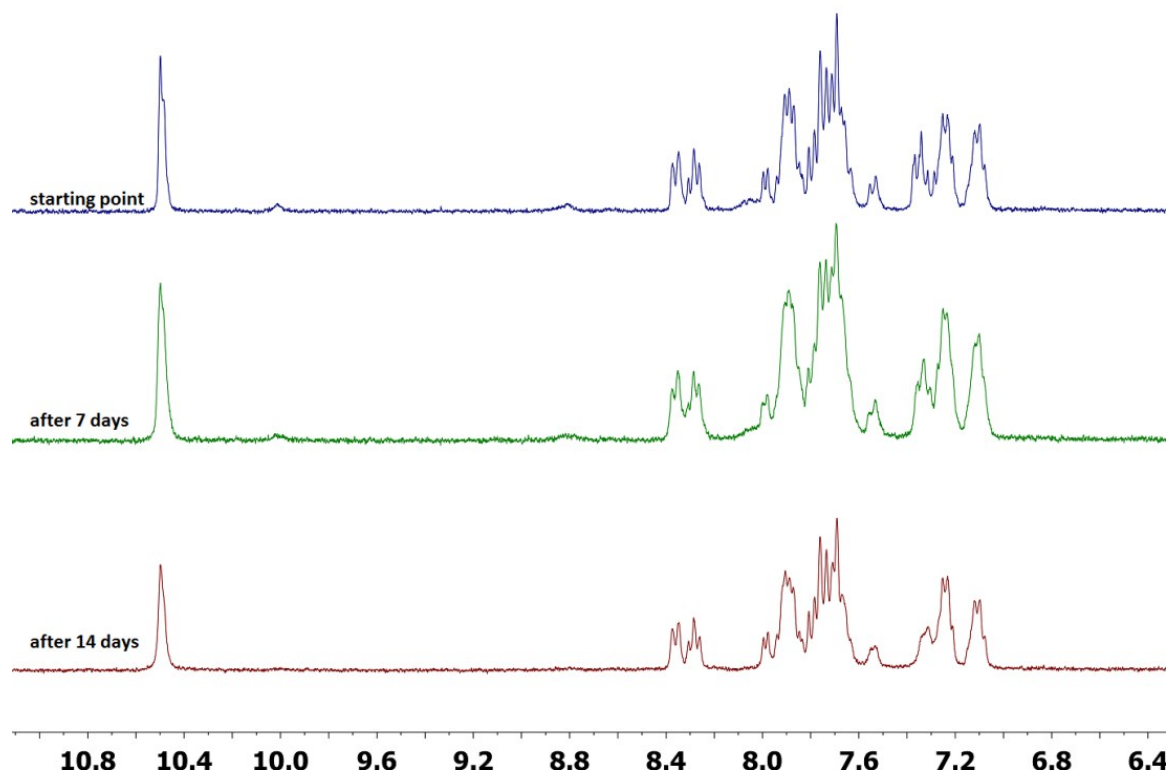


Figure S8: Long term stability of the $[\text{Fe}^{\text{II}}(\text{L})_2](\text{ClO}_4)_2$ complex followed by ^1H NMR (300 MHz CD_3CN) spectra recorded in the absence of oxygen.

2. Mass Spectrometry Data

Acquisition Parameter

Source Type	ESI	Ion Polarity	Positive	Set Nebulizer	0.3 Bar
Focus	Active	Set Capillary	3600 V	Set Dry Heater	200 °C
Scan Begin	50 m/z	Set End Plate Offset	-500 V	Set Dry Gas	4.0 l/min
Scan End	1200 m/z	Set Charging Voltage	2000 V	Set Divert Valve	Source
		Set Corona	0 nA	Set APCI Heater	0 °C

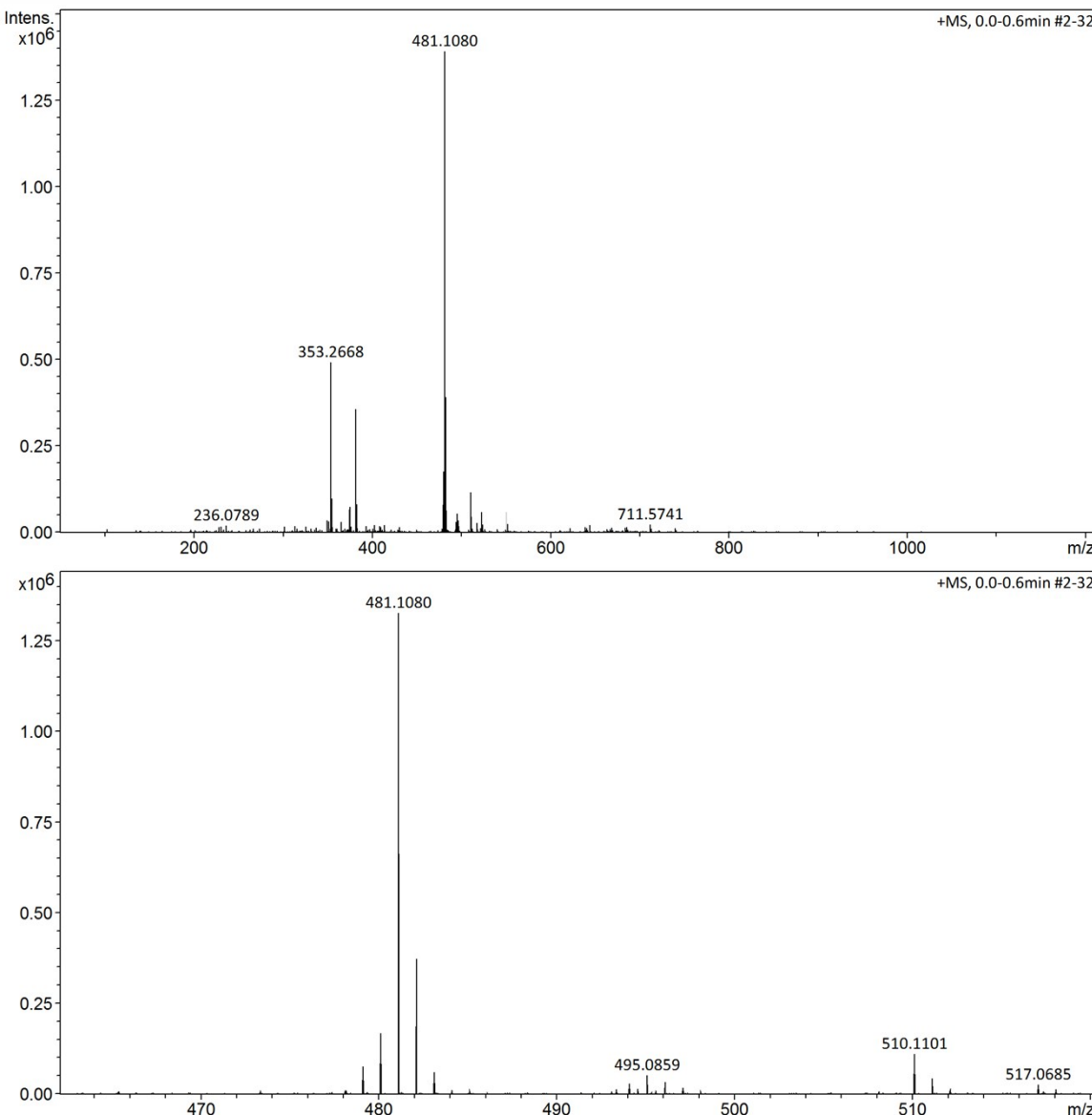


Figure S9. ESI-TOF MS spectrum of $[\text{Fe}^{\text{II}}(\text{L})_2](\text{ClO}_4)_2$. Calc. $\{[\text{Fe}^{\text{II}}(\text{L})_2]-\text{H}\}^+$ 481.107 m/z. Found 481.1080 m/z.

Acquisition Parameter

Source Type	ESI	Ion Polarity	Positive	Set Nebulizer	0.3 Bar
Focus	Active	Set Capillary	5500 V	Set Dry Heater	200 °C
Scan Begin	50 m/z	Set End Plate Offset	-500 V	Set Dry Gas	4.0 l/min
Scan End	650 m/z	Set Charging Voltage	2000 V	Set Divert Valve	Source
		Set Corona	0 nA	Set APCI Heater	0 °C

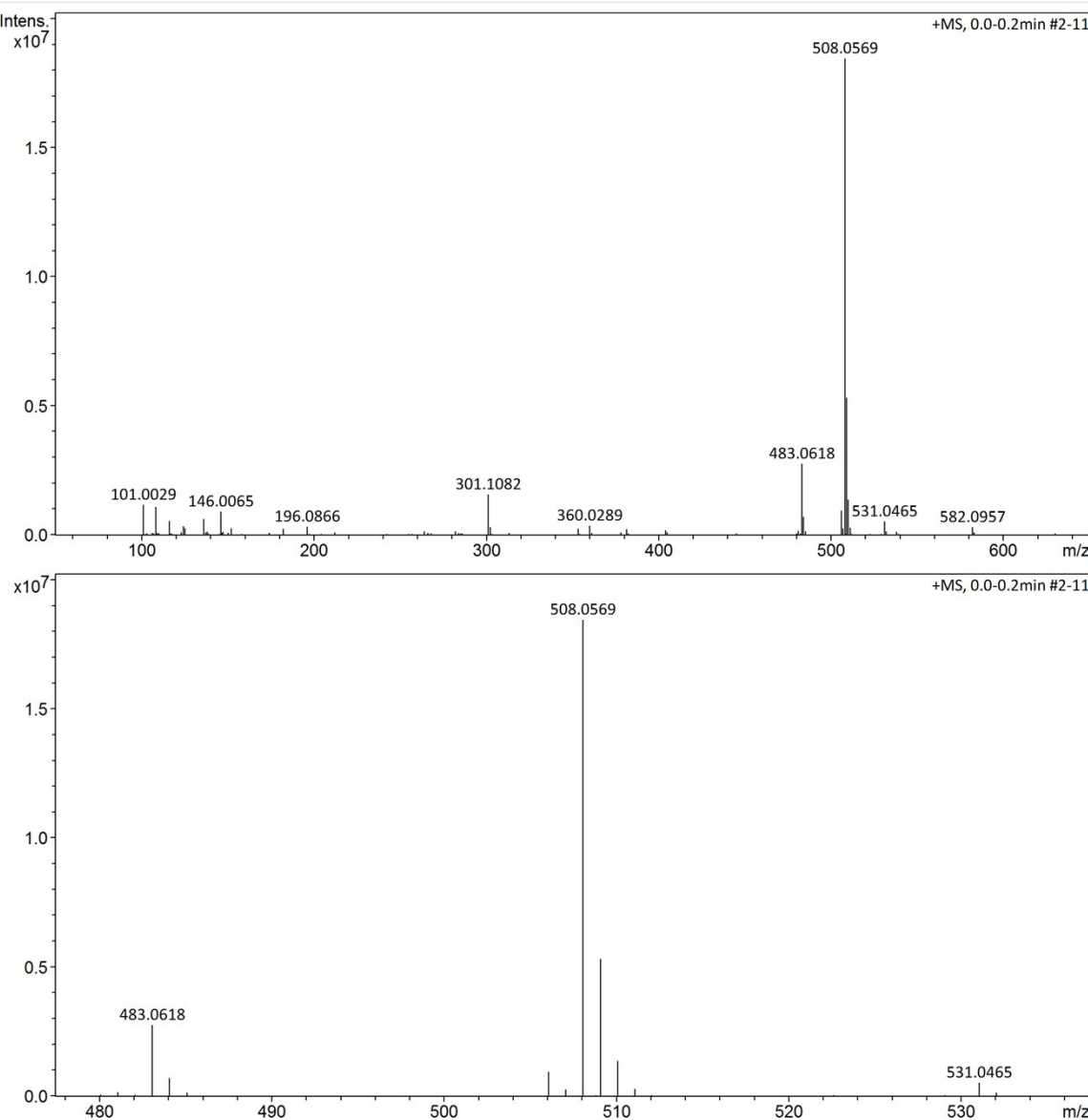


Figure 10. ESI-TOF MS spectrum of $[\text{Fe}^{\text{III}}(\text{L}^{\text{ox}}\text{-H})_2]\text{ClO}_4$. Calc. $[\text{Fe}^{\text{III}}(\text{L}^{\text{ox}}\text{-H})_2]^+$ 508.058 m/z. Found 508.0569 m/z.

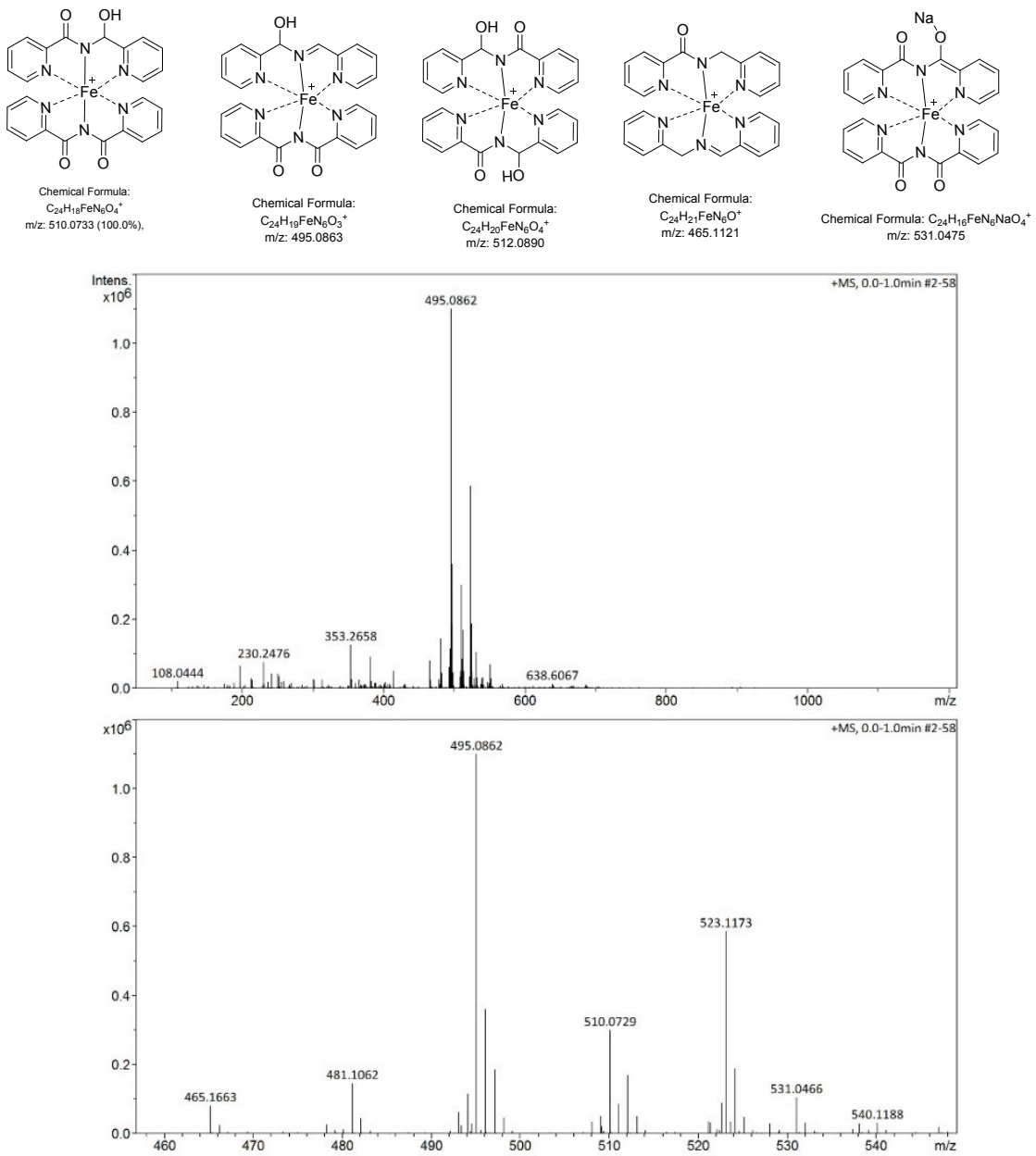


Figure S11. ESI-TOF-MS spectra of the oxidation intermediates found in crystallisation solution (ethanol) and their chemical structures.

3. UV-Vis data

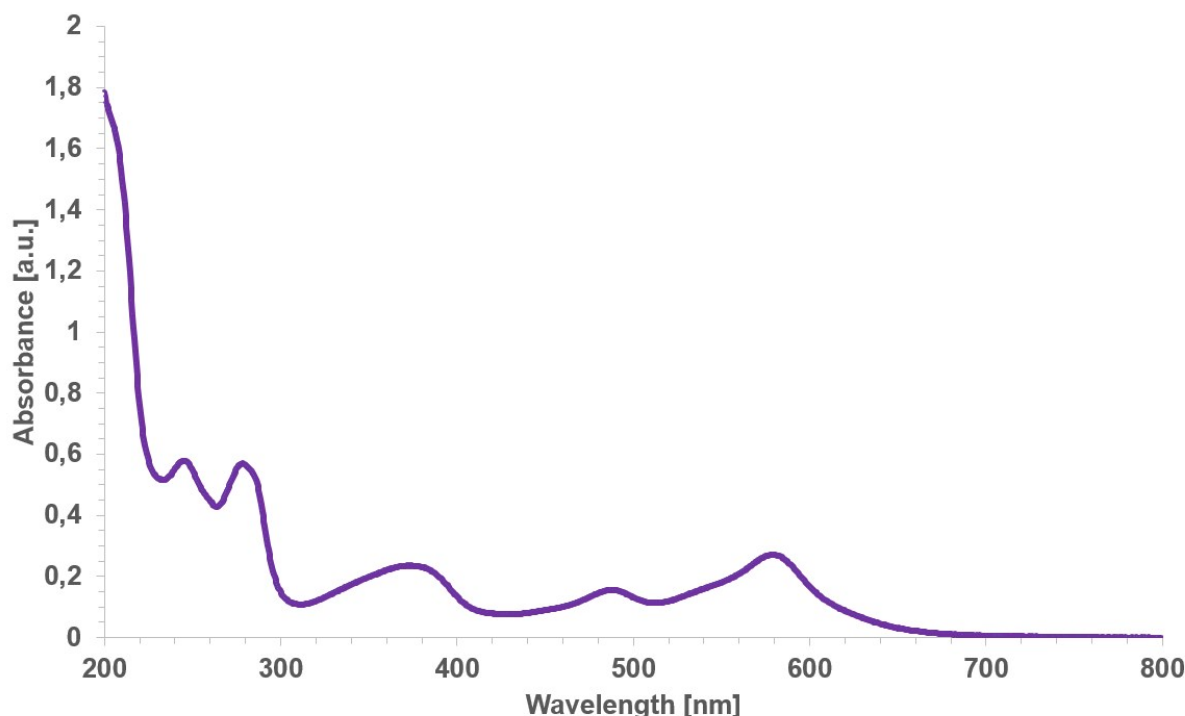


Figure S12. UV-Vis spectrum (MeCN solution) of $[\text{Fe}^{\text{II}}(\text{L})_2](\text{ClO}_4)_2$.

4. Elemental Analysis data

Table S1. Elemental analysis

$[\text{Fe}^{\text{II}}(\text{L})_2](\text{ClO}_4)_2 \cdot 2\text{H}_2\text{O}$

Calc. for $\text{C}_{24}\text{H}_{26}\text{Cl}_2\text{FeN}_6\text{O}_{12}$ C: 40.19; H: 3.65; N: 11.72;
Found 1: C: 40.16; H: 3.74; N: 11.78;
Found 2: C: 40.24; H: 3.64; N: 11.69;
Found 3: C: 40.18; H: 3.71; N: 11.79;

$[\text{Fe}^{\text{III}}(\text{L}^{\text{ox-H}})_2]\text{ClO}_4 \cdot \text{C}_2\text{H}_5\text{OH}$

Calc. for $\text{C}_{26}\text{H}_{22}\text{ClFeN}_6\text{O}_9$ C: 47.76; H: 3.39; N: 12.85;
Found 1: C: 47.70; H: 3.44; N: 12.91;
Found 2: C: 47.67; H: 3.58; N: 12.74;
Found 3: C: 47.84; H: 3.50; N: 12.78;

5. Crystallographic data

Suitable single crystals for X-ray analysis were obtained by slow evaporation from ethanol. Data was collected on a 4-circle Xcalibur EosS2 diffractometer (Agilent Technologies) equipped with a CCD detector. X-ray data was collected at room temperature using graphite-monochromated Mo K α radiation ($\lambda_{\alpha} = 0.71073 \text{ \AA}$) with the ω -scan technique. For data reduction, UB-matrix determination and absorption correction CrysAlisPro software was used¹. Using Olex2², the structure was solved by direct methods using ShelXL³, and refined by full-matrix least-squares against F2 utilizing with the program SHELXL⁴. All non-hydrogen atoms were refined anisotropically. Hydrogen atoms were located in idealized positions by molecular geometry and refined as rigid groups. Uiso of hydrogen atoms were set as 1.2 (for C-carries) and 1.5 (for O-carriers) times Ueq of the corresponding carrier atom. Selected structural parameters are reported in Table 1. Structure of $[\text{Fe}^{\text{III}}(\text{L}^{\text{ox}}-\text{H})_2]\text{ClO}_4$ contain solvent accessible voids with small amount of solvent molecule(s) used for recrystallization. As they could not be modelled satisfactorily data were treated with the solvent mask in Olex2. Single-crystal structure analysis reveals that $[\text{Fe}^{\text{III}}(\text{L}^{\text{ox}}-\text{H})_2]\text{ClO}_4$ crystallizes in the triclinic system P-1 space group. The Fe(III) ion is six-coordinated showing an almost perfected octahedral coordination geometry.

Table S2 Crystal data and structure refinement for $[\text{Fe}^{\text{III}}(\text{L}^{\text{ox}}-\text{H})_2]\text{ClO}_4$.

Identification code	Radiation MoK α ($\lambda = 0.71073$)
Empirical formula C24H16ClFeN6O8	2 Θ range for data collection/° 8.206 to 50.048
Formula weight 607.73	Index ranges -10 ≤ h ≤ 10, -14 ≤ k ≤ 14, -15 ≤ l ≤ 16
Temperature/K 293(2)	Reflections collected 41842
Crystal system triclinic	Independent reflections 4442 [Rint = 0.0664, Rsigma = 0.0396]
Space group P-1	Data/restraints/para meters 4442/0/361
a/ \AA 8.9536(2)	Goodness-of-fit on F2 1.065
b/ \AA 11.9966(3)	Final R indexes [$I >= 2\sigma$ (I)] R1 = 0.0480, wR2 = 0.1295
c/ \AA 13.8709(3)	Final R indexes [all data] R1 = 0.0612, wR2 = 0.1373
α /° 107.694(2)	Largest diff.
β /° 105.087(2)	peak/hole / e \AA^{-3} 0.49/-0.43
γ /° 99.040(2)	
Volume/ \AA^3 1324.54(6)	
Z 2	
pcccg/cm ³ 1.524	
μ/mm^{-1} 0.730	
F(000) 618.0	
Crystal size/mm ³ 0.3 × 0.2 × 0.1	

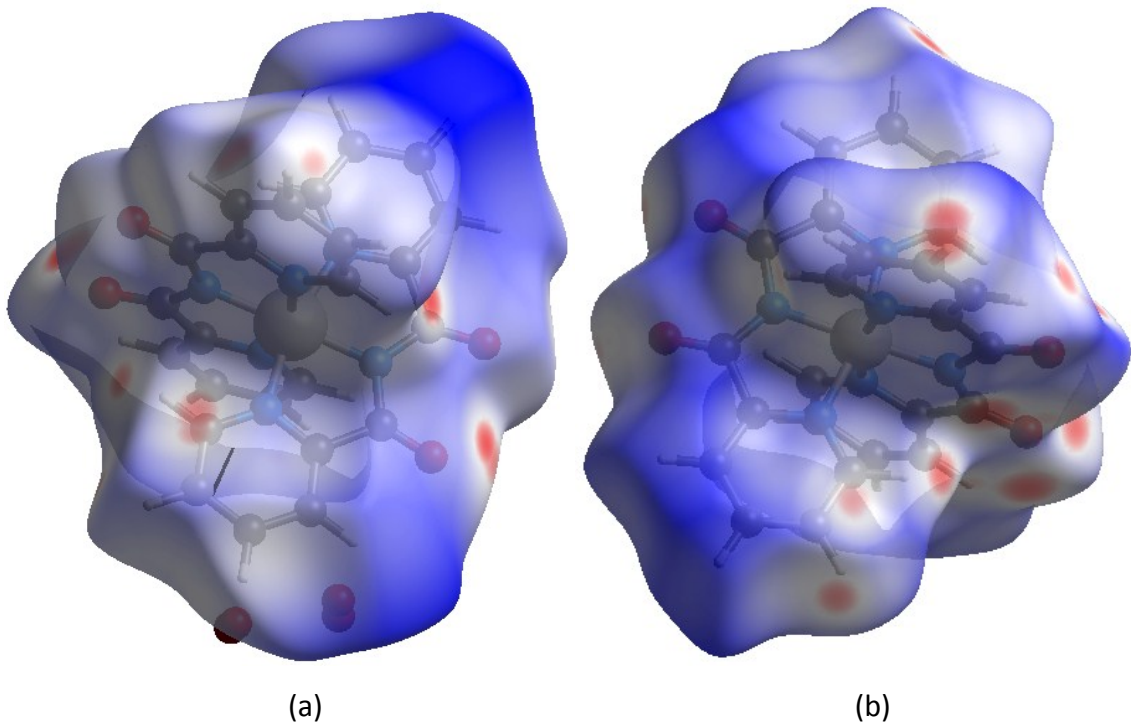


Figure S13 Hirshfeld surface representations (viewed down a) for (a) $[\text{Fe}^{\text{III}}(\text{L}^{\text{ox}}\text{-H})_2]\text{ClO}_4$ ($= [\text{Fe}(\text{bpca})_2]\text{ClO}_4$) and (b) $[\text{Co}(\text{bpca})_2]\text{ClO}_4 \cdot \text{CH}_3\text{OH}$,⁵ CCDC 187392. Red regions indicate points where interaction with an adjacent atom exceeds that of dispersion; in both cases, the atoms adjacent to the oxygen centres are aromatic hydrogen.

6. Supplementary References

1. Oxford Diffraction, Oxford Diffraction Ltd., Xcalibur CCD system, CrysAlis Software system, Version 1.171, **2004**.
2. O. V. Dolomanov, L. J. Bourhis, R. J. Gildea, J. A. K. Howard, and H. Puschmann, *J. Appl. Cryst.* 2009, **42**, 339-341.
3. G. M. Sheldrick, *Acta Cryst. A* 2015, **71**, 3-8.
4. G. M. Sheldrick, *Acta Cryst. C* 2015, **71**, 3-8.
5. J. M. Rowland, M. M. Olmstead and P. K. Mascharak, *Inorg. Chem.* 2002, **41**, 2754-2760.